

Genomic integration of E. coli NADH insensitive cs and S.typhimurium Na⁺ dependent citrate transporter operon in fluorescent pseudomonads using Mini-Tn7 transposon site specific integration system and study their effects on glucose metabolism.



CHAPTER 5

5 CHAPTER

5.1 INTRODUCTION

5.1.1 Low copy number plasmid Vs high copy number plasmid based expression

Multicopy plasmids are used as a tool for recombinant gene expression, particularly the over-expression of genes. The advantages of these vectors over low copy plasmid vectors are - they are typically small (~5 kb) and high copy number results in good expression of the recombinant genes in the host organism. However, high copy number vectors also have disadvantages as the recombinant vector may be structurally or segregationally unstable (1984; O'Connor et al., 1989; Balbas and Bolivar, 1990). Most plasmids are known to cause metabolic burden on the cell and significant shift in the normal metabolism depending on the host organism, plasmid nature, and environmental conditions (Glick 1995; McLoughlin, 1994; Buch et al., 2010b; Sharma et al., 2011). This metabolic burden has been attributed to the increased demand for nucleotides for replication of plasmid DNA and translation of plasmid-encoded genes (Bimbaum and Bailey, 1991; Vind et al., 1993; Jones et al., 2000).

The maintenance of plasmid DNA in *E. coli* has been demonstrated to have diverse effects on the physiology and cellular metabolism including alteration in ATP biosynthesis as well as perturbations in host DNA replication, transcription, and translation (Rozkov et al. 2004; Ow et al. 2006; Wang et al. 2006; Chou 2007; Ow et al. 2009;). Presence of *colE1* based plasmid has been demonstrated to significantly alter several metabolic pathways in *E. coli* depending on the growth conditions. Presence of plasmids adversely affected the growth and gluconic acid secretion of phosphate solubilizing *Enterobacter asburiae* PSI3 under phosphorus limited condition (Sharma et al. 2011). Similarly, other hosts like *E. asburiae* PSI3, *Azotobacter vinelandii*, *Azospirillum brasilense*, and *Pseudomonas putida* GR12-2 also showed impaired growth, phosphate solubilization, nitrogen fixation, siderophore production, and indole acetic acid biosynthesis, under various experimental conditions (Glick 1995; Sharma et al. 2011), while in *P. chlororaphis* and *P. fluorescens* WCS365

showed reduced competitiveness and variable stability, respectively, under rhizospheric conditions (Eisenlohr and Baron 2003). PGPR traits that have been shown to be adversely affected by metabolic load include environmental fitness in soils, indole acetic acid (IAA) production (De Leij et al., 1998; Holguin and Glick, 2001), competitiveness in rhizosphere colonization and nitrogen fixation (Eisenlohr and Baron, 2003). These disadvantages suggests that multi- copy plasmids may not be the best option for metabolic engineering applications, even when the objective is to increase the intracellular concentration of an enzyme in order to improve the product concentration and flux through an existing pathway.

Low-copy plasmids may reduce the specific activity of the gene product but can compensate on the productivity by reducing the burden effects associated with high plasmid copy number while allowing the use of strong promoters to maximize gene expression. Chromosomal insertion of genes into bacterial genome is an alternative to introduction of foreign genes on plasmid and this may cause less metabolic burden.

5.1.2 Genomic integration: single copy gene insertion using mini Tn7 transposon

The mini-Tn7 transposon is a great tool for single copy tagging of bacteria in a site-specific manner at a unique and neutral site without any deleterious effects. The Tn7 transposon was originally discovered by Barth et al., (1976) on the plasmid R483 (IncI α) as an element carrying the resistance genes trimethoprim (Tm^R) and streptomycin/spectinomycin (Sm^R / Sp^R), which could be transposed to other replicons. The Tn7 transposon is of 14 kb encodes for five genes involved in the transposition process (**Fig.5.1**). These genes are flanked by the ends of the transposon, named the left (Tn7L) and the right (Tn7R) end (Lichtenstein and Brenner, 1982; Rogers et al., 1986). The Tn7 transposition process has been studied intensively in *Escherichia coli* in which Tn7 inserts with high efficiency and unique orientation into one specific location named the attTn7 site. This site of insertion is located just downstream of the coding region, in the transcriptional terminator, of the *glmS* gene and thereby does not disrupt the gene (Gringauz, et al., 1988). The *glmS* gene encodes a glucosamine synthetase, which is required for cell wall synthesis

(Volger et al., 1989). It is conserved among many bacteria and therefore Tn7 is likely to have the same specific insertion site in many different bacteria, some have already been tested (Fig. 5.1, Table 5.1). The transposon genes required for specific insertion into the attTn7 site, are tnsABCD, and they function in *trans*. Thus, sequences located in the 3' end of the coding region of *glmS* are recognised by transposase proteins directing the actual insertion into the attTn7 site, down-stream of the *glmS* gene. However, if this site is unavailable the transposon can insert into other sites with low frequency (Peters, J. E. et al., 2001).

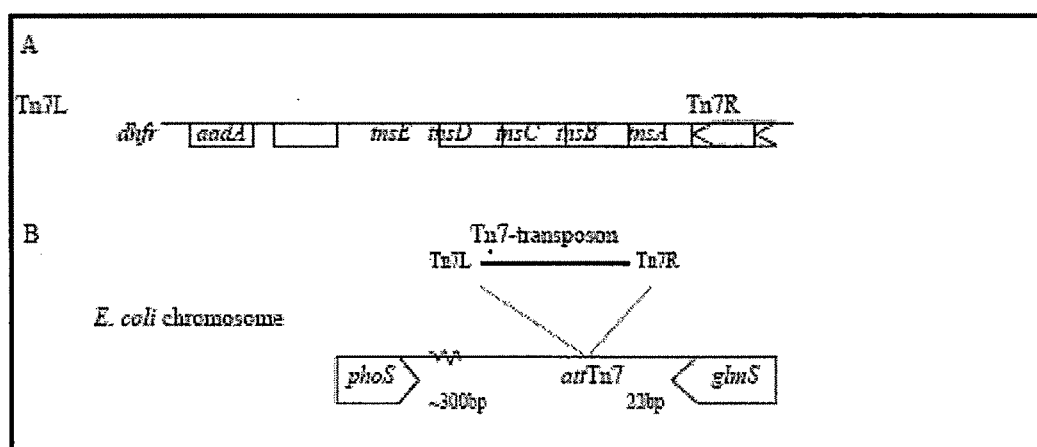


Figure 5.1: Map of transposon Tn7 (A) and its insertion site attTn7 in *Escherichia coli* (B). The gene *dhfr* encodes dihydrofolate reductase providing trimethoprim resistance and *aadA* encodes adenylyltransferase, which provides resistance to streptomycin and spectinomycin (the figure is redrawn from Craig et al., 1989).

The mini-Tn7-based gene integration system has been used for gene complementation, gene expression analysis, strain construction, and reporter gene-tagging of *Pseudomonas aeruginosa* and *Yersinia pestis*, particularly in biofilm and animal models. Heterologous genes including *lacZ* (β -galactosidase), *est* (esterase), and *gfp* (green fluorescent protein) under the control of the methanol dehydrogenase promoter have been integrated into the intergenic region between *glmS* and *dhaT* via the delivery of mini-Tn7 in *Methylobacterium extorquens*. A gene encoding for different fluorescent protein and luciferase protein along with promoter was integrated into the chromosomes of *Erwinia chrysanthemi*, *Pseudomonas fluorescens*, *Pseudomonas syringae*, and *Pseudomonas*

putida and many gram negative bacteria by the Tn7-based delivery system (Fig. 5.2) (Koch et al., 2001, Lambersten et al., 2004, Hee et al., 2008). This gene delivery system developed was applied to other organisms, such as *Burkholderia* spp. and *Proteus mirabilis*, which were determined to have multiple *glmS*-linked attTn7 sites and secondary, non-*glmS*-linked attTn7 site, respectively. Thus mini Tn7 transposition is a powerful technique for the integration or excision of a gene of interest at a single-copy on the chromosomal level, which makes it possible to conduct a variety of experiments, including insertional random mutagenesis, gene expression analysis, protein functional studies, or the gene-tagging of bacteria in living organisms.

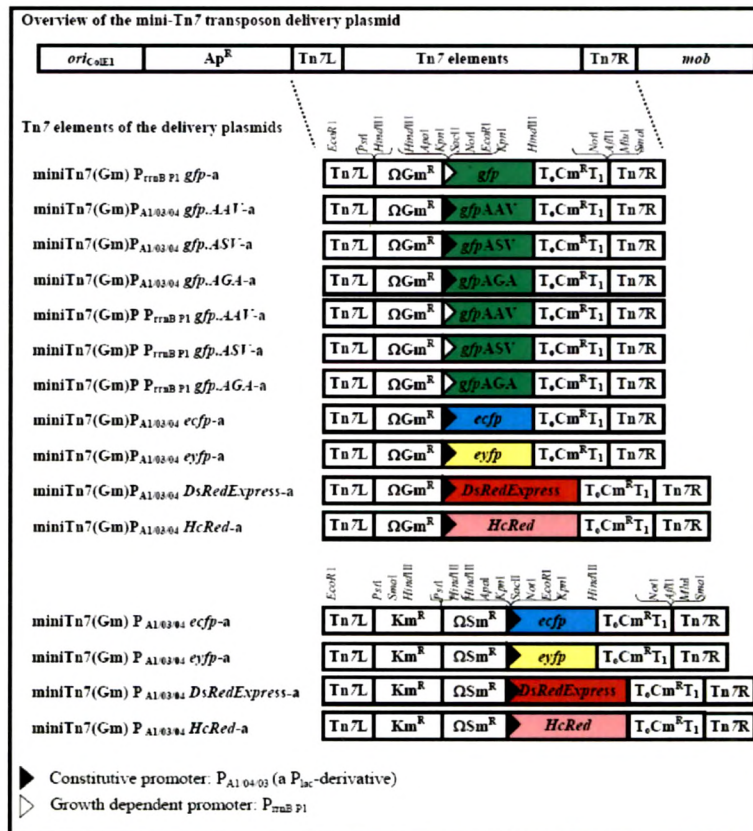


Figure 5.2: The Tn7 delivery plasmids. The resistance genes are: gentamicin resistance (Gm^R) provided by aacC1 encoding acetyltransferase-3-I(Cm^R) provided by cat encoding chloramphenicol-acetyl-transferase, kanamycin resistance (Km^R) provided by neomycin phosphotransferase (nptII), all plasmids are based on pUC19 and carry resistance to ampicillin. Ω shows that the resistance gene is flanked by transcription and

translation terminators (Fellay et al., 1987). All constructs contain the ribosomal binding site, RBSII, in front of the fluorescent gene and terminator T₀ and T₁ flanking *cat*. (Koch et al., 2001)

Table 5.1: Literature overview of bacteria tested for insertion of Tn7 (Lambertsen, 2004 supplementary data)

Bacterium	Specific insertion	Test	Bacterium	Specific insertion	Test
<i>Caulobacter crescentus</i>	Yes	Southern	<i>Pseudomonas aeruginosa</i> PAO1	Yes	Southern
<i>Desulfovibrio desulfuricans</i> G20	Yes	Southern	<i>Pseudomonas aeruginosa</i> PAOE1A	-	-
<i>Escherichia coli</i>	Yes	Southern	<i>Pseudomonas corrugate</i> strain 2140	-	Southern
<i>Escherichia coli</i> BE6	-	-	<i>Pseudomonas fluorescens</i> 701E1	Yes	Southern
<i>Erwinia chrysanthemi</i> EC16	Yes	Southern	<i>Pseudomonas fluorescens</i> DR54	Yes	PCR
<i>Klebsiella pneumonia</i>	-	-	<i>Pseudomonas putida</i> KT2440	Yes	PCR, Southern
<i>Methylophilus methylotrophus</i>	-	-	<i>Pseudomonas putida</i> GR12-2	Yes	Southern
<i>P. fluorescens</i> CHA0	Yes	Southern	<i>Pseudomonas putida</i> R20	No	Southern
<i>Pseudomonas</i> DS-S73	Yes	-	<i>Pseudomonas putida</i> PH6	No	Southern
<i>Pseudomonas</i> S108	Yes	-	<i>Pseudomonas solanacearum</i>	Yes	Southern
<i>Pseudomonas aeruginosa</i> PAC and PAO1161	Yes	Southern	<i>Pseudomonas syringae</i> pv. <i>glycinea</i> PsgR4	Yes	Southern
			<i>Rhodospirillum rubrum</i>	-	Southern

Bacterium	Specific insertion	Test
<i>Salmonella typhimurium</i>	-	-
<i>Serratia marcescens</i>	-	-
<i>Sphingomonas yanoikuyae</i> B1	Yes	Southern
<i>Xanthomonas campestris</i> pv. <i>campestris</i> NC PPB 1145	Yes	Southern

The present study describes the genomic integration of *E. coli* NADH insensitive *cs* Y145F and *S. typhimurium* sodium citrate transporter *citC* gene into fluorescent

pseudomonads genome and compares its effect to plasmid based expression on glucose catabolism and citric acid secretion. All the experiments were carried out in buffered Tris HCl (pH8.2) minimal medium in phosphate deficient condition mimicking the soil environment.

5.2 WORK PLAN

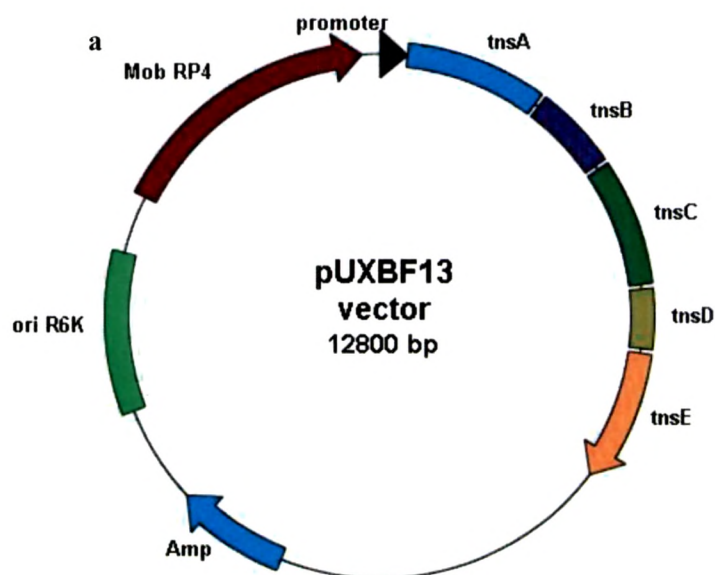
The experimental plan of work includes the following-

5.2.1 Bacterial strains used in the study

Table 5.2: Wild type and recombinant strains used in the study.

Bacterial strains/Plasmids	Characteristics	Source/Reference
<i>E. coli</i> DH5 α	F- ϕ 80 Δ lacZ Δ M15 Δ (lacZYA-argF) U169 <i>recA1 endA1 hsdR17</i> (rk $^-$, mk $^+$) <i>phoA supE44 λ-thi-1 gyrA96 relA1</i>	Sambrook and Russell, 2001
SM101 AKN68	<i>E. coli</i> SM101:: λ pir helper plasmid pUXBF13 providing the Tn7 transposes proteins Amp r	A generous gift of Prof. Soren Molin, DTU, Denmark
JM101 AKN69	<i>E. coli</i> JM101 containing miniTn7(Gm) P _{AI704/03} -eyfp plasmid Gm r , Cm r	A generous gift of Prof. Soren Molin, DTU, Denmark
<i>E. coli</i> DH5 α pYCIInt	<i>E. coli</i> DH5 α containing <i>yc</i> operon in mini Tn7 delivery plasmid AKN69 under <i>plac</i>	This Chapter
<i>P. fluorescens</i> PIO-1	Wild type strain	A generous gift of Prof. Mark Sylvi, USA
<i>P. fluorescens</i> Pf-5	Wild type strain	A generous gift of Prof. L. Thomashow USA

<i>P. fluorescens</i> CHAO-1	Wild type strain	
<i>P. fluorescens</i> ATCC13525	Wild type strain	ATCC
<i>P. fluorescens</i> P109	Wild type strain	A generous gift of Prof. B. N. Johri
<i>P. fluorescens</i> Fp315	Wild type strain	A generous gift of Prof. B. N. Johri
<i>Pf</i> (pGm)	<i>P. fluorescens</i> strain with pUCPM18; Gm ^r	Ch3
<i>Pf</i> (pYC)	<i>P. fluorescens</i> strains with pYC; Gm ^r	Ch4
<i>Pf</i> (Int)	<i>P. fluorescens</i> strains genomic integrant, Gm ^r	This Chapter



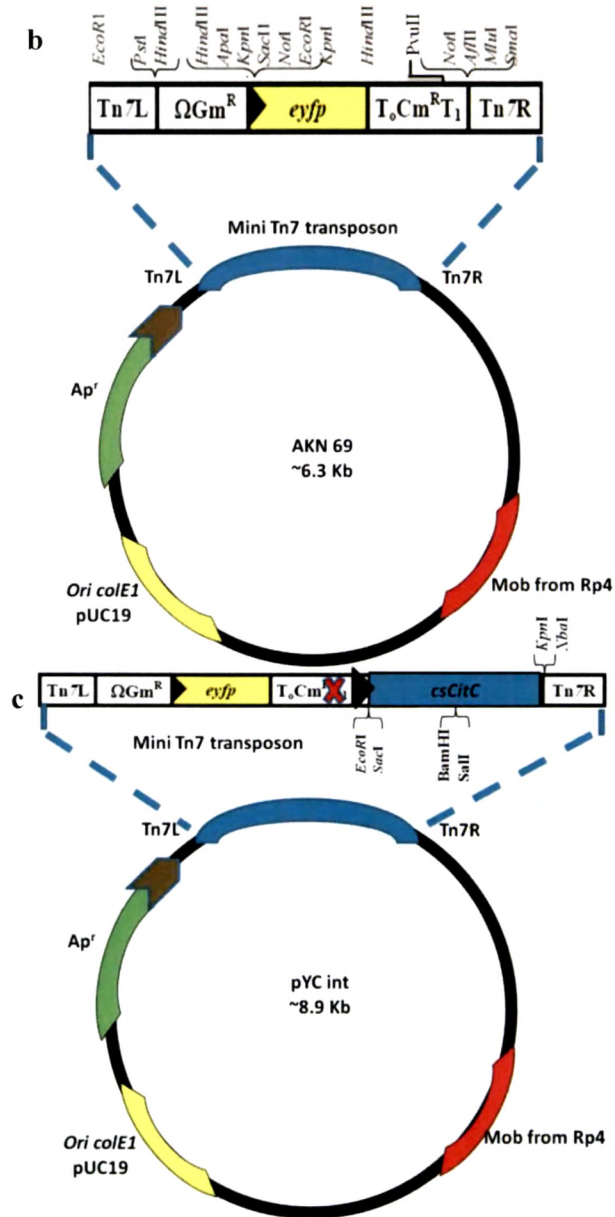


Figure 5.3: Vector map of mini tn7 helper plasmid (a), mini tn7 delivery plasmid (b), and mini tn7 delivery plasmid with *yc* gene cloned along with *plac* (c).

5.2.2 Recombinant plasmid construction and genomic integration

The strategy for construction of mini Tn7 delivery plasmid containing *yc* gene under *plac* and insertion into *P. fluorescens* genome is depicted in Fig. 5.4.

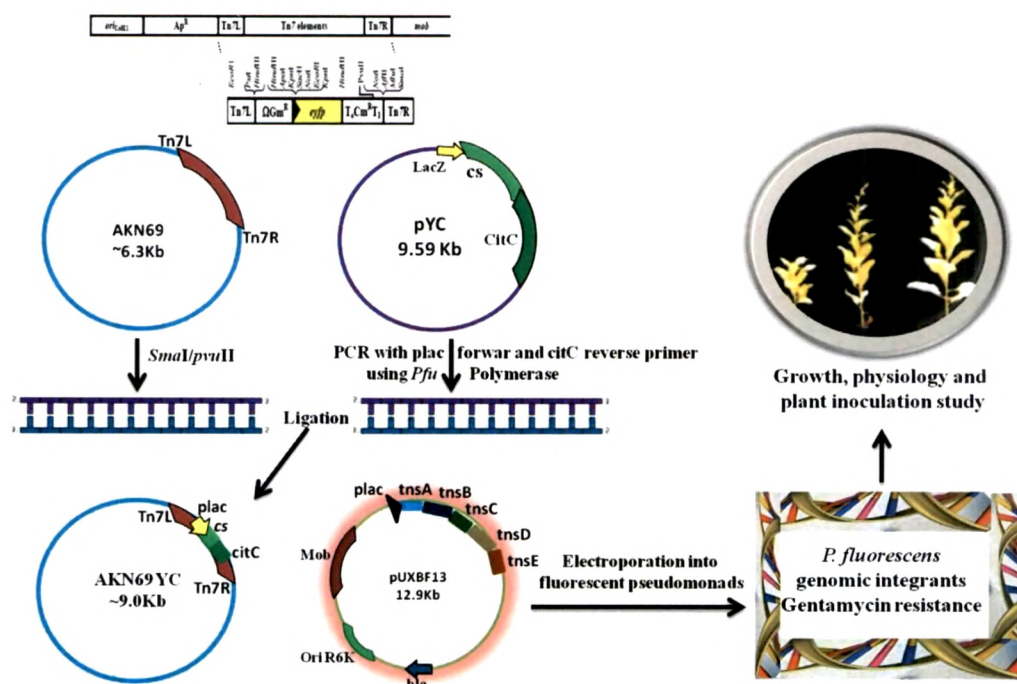


Figure 5.4: Strategy for cloning and genomic integration.

yc operon along with *plac* is amplified using *plac* forward primer and *citC* gene reverse primer from pYC plasmid using high fidelity *taq* polymerase to obtain blunt end product. Cloning of isolated *citC* gene was carried out in AKN 69 t vector using *SmaI* site after disruption of chloramphenicol resistance gene using *PvuII* enzyme. The clone was confirmed by double digestion with *EcoRI-XbaI* restriction site. Functional confirmation of the recombinant plasmid was done by growing *E. coli* DH5 containing pYCint on Koser citrate broth containing citric acid as a sole carbon source supplemented with 100mg/ml thymine and 0.1mM IPTG.

The mini Tn7 recombinant plasmid along with pUXBF13 containing the transposase genes is delivered into *P. fluorescens* strains by the electroporation method as described by Choi et al. (2006). For preparation of electrocompetent cell, 6 ml culture of *P. fluorescens* strains were grown overnight in LB medium at 30°C with shaking (225rpm) in a sterile 25 ml conical flask. The whole culture is then evenly distributed into four sterile micro centrifuge tubes and centrifuged at 16,000g and room temperature for 2 min, using a sterile 1-ml disposable pipette tip, the supernatant were dispensed and discarded into a biological waste container. Each cell pellet is suspended in 1 ml of 300 mM sucrose (kept at room temperature) and centrifuged as mentioned earlier. Cultures were pipetted carefully to avoid aerosolization of pathogenic bacteria and/or contamination of the pipette. Plugged pipette tips were used to avoid contamination of the pipette. The sucrose solution was stored at room temperature because cold sucrose resulted in greatly reduced transformation competency. The supernatant was discarded and each cell pellet was suspended in 1 ml of 300 mM sucrose and centrifuged. Finally, the four cell pellets were resuspended in a combined volume of 200 μ l of 300 mM sucrose. This was sufficient for two electroporations. 100 μ l of electrocompetent cells were transferred aseptically to a 2-mm gap-width electroporation cuvette. Using a 1–100 μ l gel-loading tip, 50 ng each of mini-Tn7 element DNA (pYCInt and pUXBF13) were added and mixed by gentle stirring with the gel-loading pipette tip to avoid air bubbles. The volume of DNA ensured not to exceed 10 μ l per 100 μ l of electrocompetent cells to avoid arcing during the electroshock. Electroporation was carried out using BioRad electroporator with the following settings: 25 μ F, 200 Ω , 2.5 kV (the time constant should be < 5 ms). Immediately 1 ml of LB medium is added and incubated with shaking (225 r.p.m.) for 1 h at 37 °C. 100 μ l of the mixture plated on an LB+Gm30 plate) and the remaining cultures were transferred to a sterile microcentrifuge tube and centrifuged at 16,000g at room temperature for 2 min. The supernatant was discarded and pellet was resuspended in 200 μ l of LB medium and plated on another LB+Gm30 plate. Plates were incubated at 37 °C overnight or until colonies have grown. 4-6 colonies from each plate were regrown on LB medium containing gentamycin and the respective cultures were streaked on pseudomonas agar plate containing gentamycin.

Preliminary confirmations of the genomic integrants were done by monitoring the growth on gentamycin plate and fluorescens and finally confirmed by PCR with gene specific primer (Table 5.3)

Table 5.3: Primer pair used for the PCR test of genomic integrants.

Name of the primer	Sequence	Annealing site	Tm
Tn7-Gm	5'ATATCGACCCAAGTACCGCC	Nt 509 from the strat site of aaC1 gene	57.4
csR	CGGGATTCCTGTTGTTAACGCTTGATATCGC	Cs gene reverse primer	59.6°C, 46.2%

5.2.3 Effect of genomic integration on physiology, biochemical properties and overall glucose catabolism of fluorescent pseudomonads

P. fluorescens genomic integrants were subjected to physiological experiments involving growth and organic acid production profiles on Tris HCl (pH 8.0) rock phosphate minimal medium with 75 mM glucose as carbon source. The samples withdrawn at regular interval were analyzed for O.D.600nm, pH, and extracellular glucose. Stationary phase cultures harvested at the time of pH drop were subjected to organic acid estimation using HPLC (Section 2.7.3). The physiological parameters were calculated as in section. The effectiveness of the genomic integrants were compared with the wild type and plasmid bearing strains of fluorescent pseudomonads. The enzyme assays (CS, G-6-PDH, ICDH, PYC, ICL and GDH) were performed with cell free extracts of late log to stationary phase cultures as described in Section.

5.3 RESULTS

5.3.1 Construction of integration delivery plasmid containing NADH insensitive *cs* Y145F and *S. tphilurium citC* operon under *lac* promoter:

The plasmid pYCint containing NADH insensitive *cs* Y145F and *S. tphilurium citC* operon under *lac* promoter was constructed in the *Sma*I site of AKN69 vector as schematically represented (Fig. 5.4). The recombinant plasmid was confirmed by restriction enzyme digestion (Fig. 5.5) and PCR (Fig. 5.6).

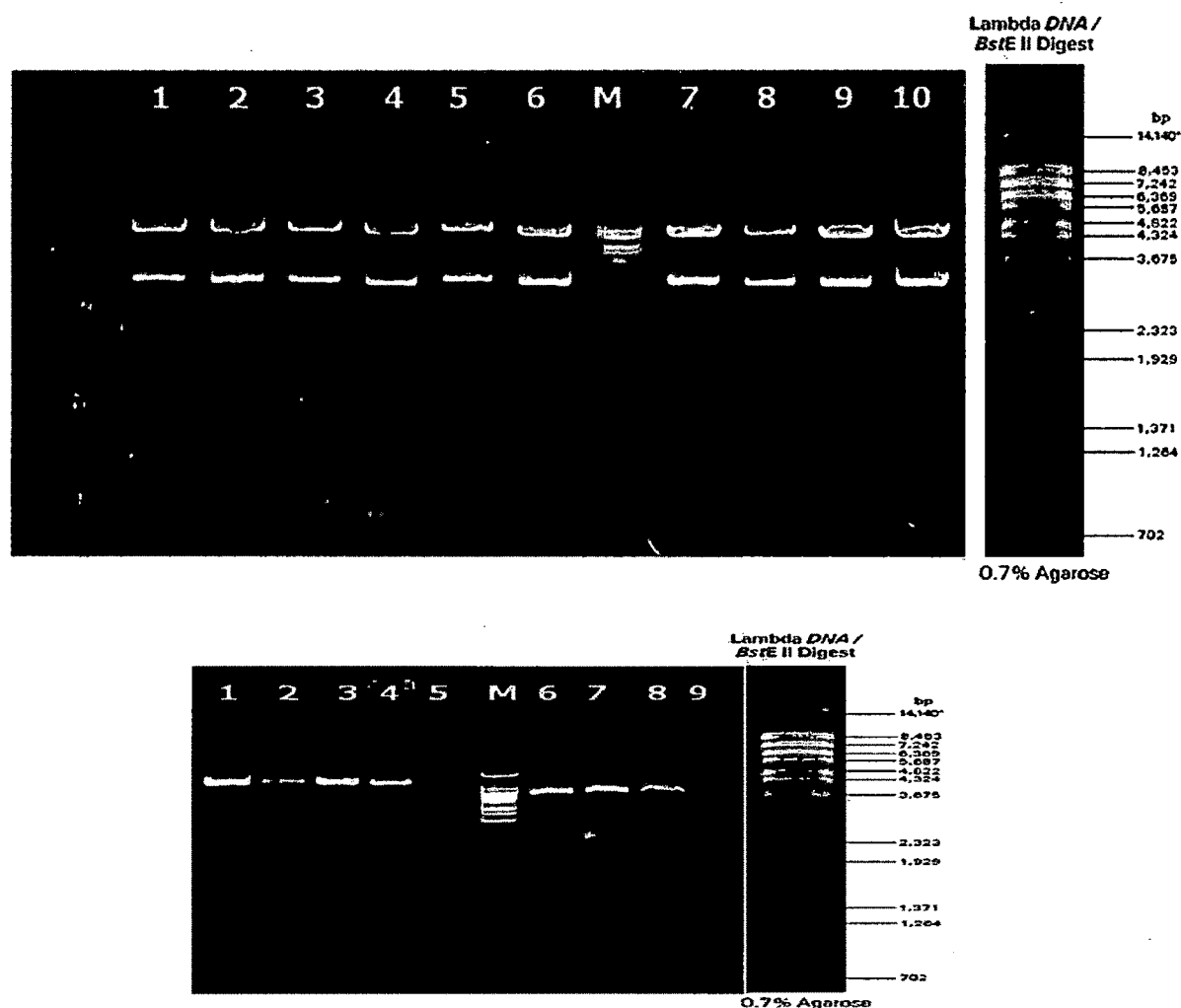


Figure 5.5: Restriction enzyme digestion pattern of pYCint plasmid containing NADH insensitive Y145F and *S. tphilurium* sodium citrate transporter operon under *lac* promoter. (A) Lane 1-10: pYCint plasmid

digested with EcoRI-XbaI (6.3Kb, 2.6kb); (B) Lane 1-4: NotI digestion pattern of pYCInt plasmid (~8.9 Kb); Lane 6-9: pYCInt plasmid digested with EcoRI-XbaI (6.3Kb, 2.6kb). Lane M: MWM lambda DNA BstEII digest.

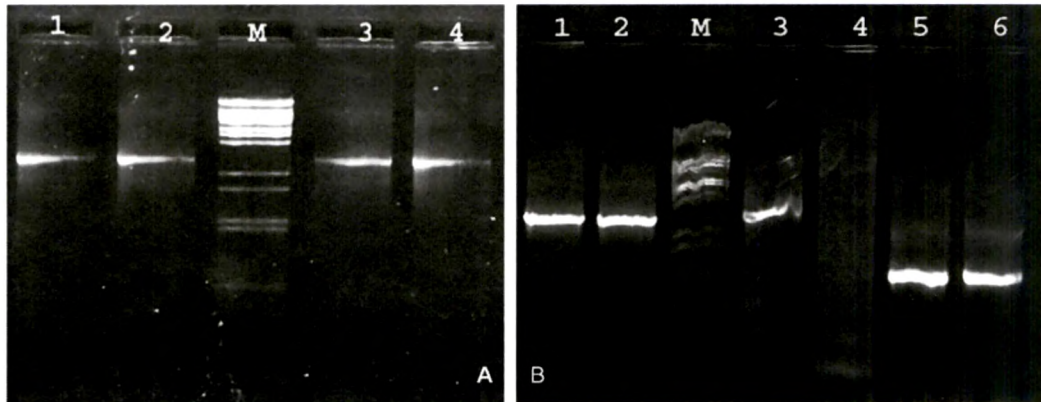


Figure 5.6: PCR amplification of *plac yc* gene cloned in integration delivery plasmid AKN69. (A) lane 1-4: *plac yc* amplicon (2.6Kb); (B) lane 1-5: *plac yc* amplicon (2.6Kb); lane 5: *cs* gene amplicon (1.28Kb); Lane 6: *citC* gene amplicon (1.34Kb). Lane M: MWM lambda DNA BstEII digests.

5.3.2 Characterization of *lacYC* operon genomic integrants of *P. fluorescens* strains.

The integration delivery plasmid inserts *plac yc* operon along with gentamycin resistance gene. Hence, when the *P. fluorescens* transformants were selected on pseudomonas agar plate containing gentamycin at 50 µg/ml, the integrants were able to grow and show fluorescence while the wild type pseudomonads failed to grow on gentamycin (Fig. 5.7). PCR of the genomic DNA using specific primer (Table 5.3) resulted in an amplicon of 2.8 kb confirming the genomic integration (Fig. 5.8).

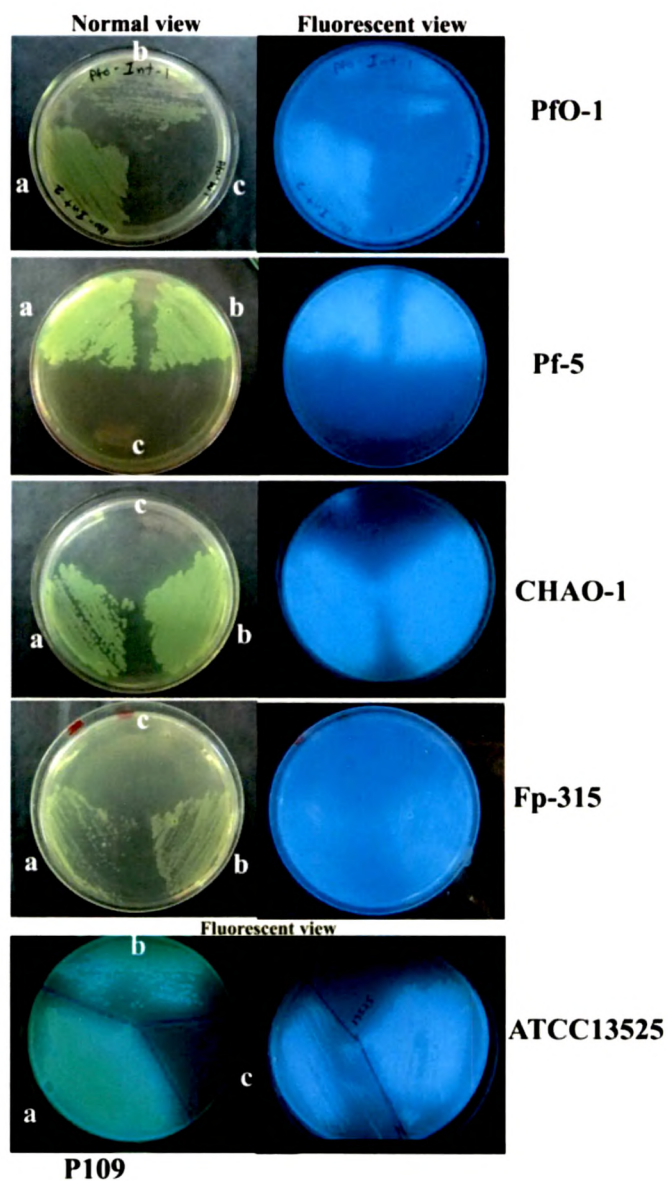


Figure 5.7: Natural fluorescence and antibiotic resistance of genomic Integrants of *P. fluorescens* PfO-1, *P. fluorescens* Pf-5, *P. fluorescens* CHAO-1, *P. fluorescens* Fp315, *P. fluorescens* P109 and *P. fluorescens* ATCC13525. Pseudomonas agar plates containing ampicillin and gentamycin each at 50 µg/ml. (a) *P. fluorescens* pYC plasmid transformants (b) *P. fluorescens* genomic integrants; (c) *P. fluorescens* wild type.

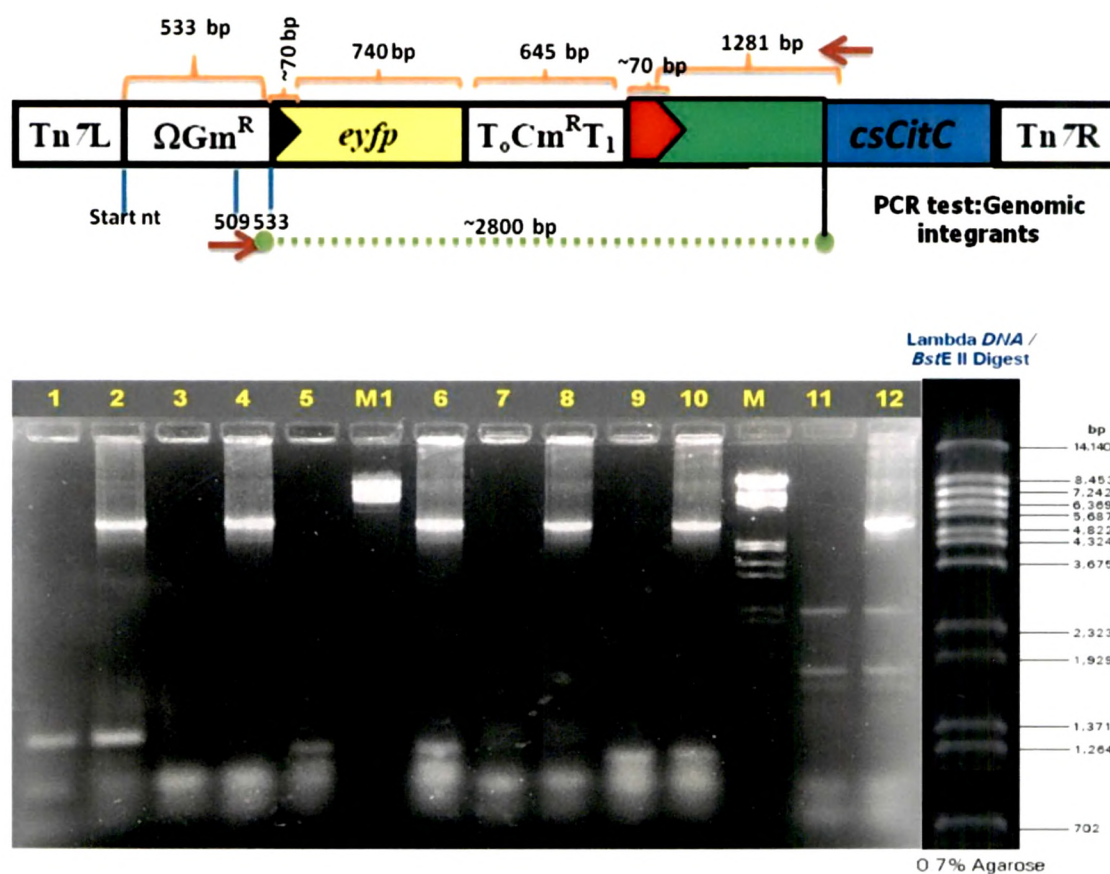
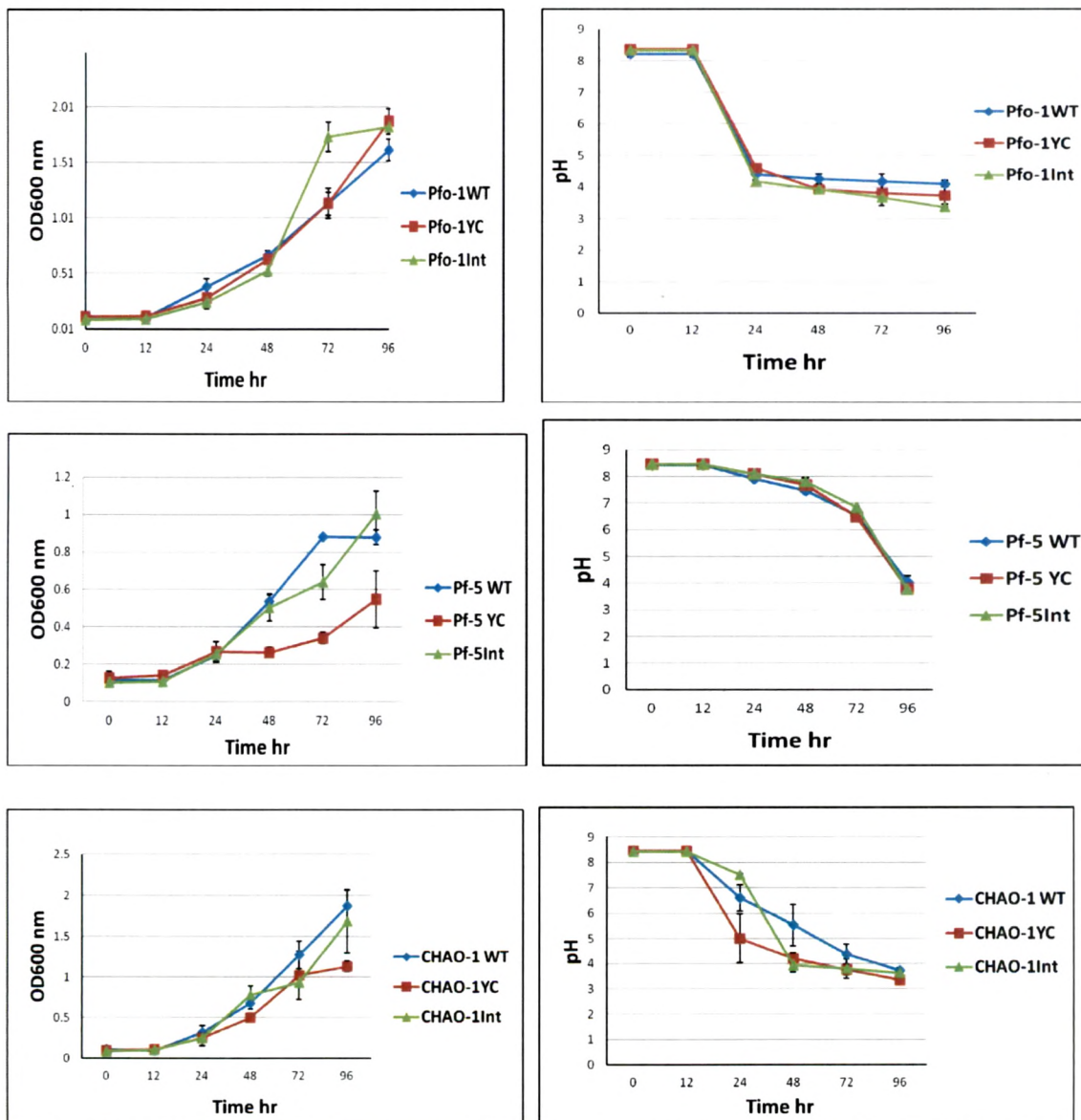


Figure 5.8: PCR test of genomic DNA isolated from *P. fluorescens* wild type and genomic integrants using Tn7-Gm (510 nt from the start site of Gm^r gene) and *cs* reverse primer (~2800 bp). Lane1: *P. fluorescens* PfO-1 WT, Lane2: *P. fluorescens* PfO-1 genomic integrant (...); Lane3: *P. fluorescens* Pf-5 WT; lane4: *P. fluorescens* Pf-5 genomic integrant; Lane 5: *P. fluorescens* CHAO-1 WT; Lane6: *P. fluorescens* CHAO-1 genomic integrant; lane 7: *P. fluorescens* ATCC13525 WT; lane8: *P. fluorescens* ATCC13525 genomic integrant; Lane 9: *P. fluorescens* P109 WT; lane10: *P. fluorescens* P109 genomic integrant; Lane11: *P. fluorescens* Fp315 WT; Lane12: *P. fluorescens* Fp315 genomic integrant. LaneM: MWM with Lambda DNA BstEII digests.

5.3.3 Physiological characterization of *P. fluorescens* *yc* operon genomic integrants.

The growth characteristics of *P. fluorescens* *yc* operon genomic integrants were determined upon grown under buffered-RP (TRP, 75mM Tris HCl pH 8.0) broth minimal medium containign75mM glucose (Fig 5.9). *P. fluorescens* Fp315 genomic integrants

showed an enhanced growth rate by 1.6 fold as compared to the plasmid transformants. Growth rate of *P. fluorescens* Pf-5 plasmid transformants drastically reduced (1.7 fold) as compared to the wild type culture and genomic integrants. But no growth difference was found with other strains. All strains acidified the medium within 72-96 hr of growth but genomic integrants of Pfo-1 and Pf5Int acidified the medium pH below 5 much faster within 48 hr.



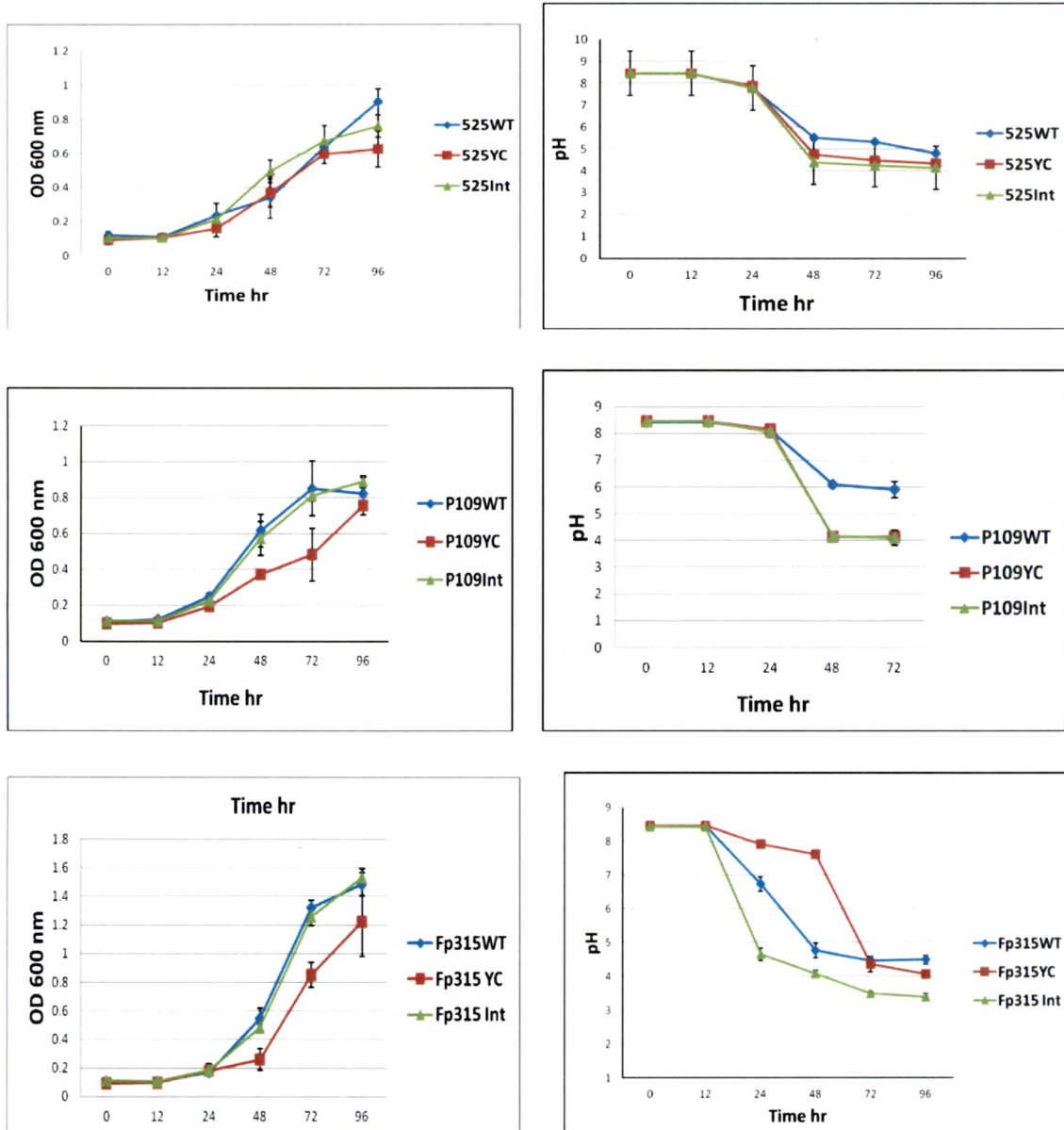


Figure 5.9: Growth profile and media acidification of genomic integrants and plasmid transformants of fluorescent pseudomonads including selected native isolates on TRP medium. The growth and media acidification were monitored on TRP medium with 75 mM tris HCl (pH 8.0), 75mM glucose and 1mg/ml RP. The values are plotted as Mean \pm S.D. of 3 independent observations.

Both qualitative and quantitative changes in total glucose utilization, glucose consumption and specific glucose utilization rate were monitored amongst the strains (Table 5.4). *P. fluorescens* CHAO-1 genomic integrants showed an increase in total amount of glucose utilized by 1.36 fold and 1.25 fold as compared to the wild type and plasmid transformant respectively, whereas *P. fluorescens* P109 genomic integrants showed a 1.3 fold decrease in the total glucose utilization.

Total glucose utilization remain unaltered in *P. fluorescens* PfO-1, Pf-5 and ATCC 13525. The amount of glucose consumed decreased by 1.57 fold and 1.3 fold as compared to wild type and Pf(pYC) in *P. fluorescens* PfO-1 genomic integrant, respectively. Similar decrease was observed in *P. fluorescens* Pf-5, ATCC13525 and Fp315 strains by 2.5, 1.26 and 2.26 respectively as compared to wild type strain. On the other hand, an increased glucose consumption by 1.26 fold and 3 fold were observed in ATCC13525 and P109 genomic integrant, respectively, as compared to wild type strain. Glucose consumption remain unaltered in *P. fluorescens* CHAO-1 genomic integrant. The biomass yield and specific glucose utilization rate were remained unaltered in *P. fluorescens* CHAO-1 and ATCC13525 genomic integrants. Biomass yield was increased by 3.5, 2.2, 2.1 and 1.7 fold in *P. fluorescens* PfO-1, Pf-5, P109 and Fp315, respectively as compared to wild type control. *P. fluorescens* Fp315 genomic integrant showed a decrease in specific glucose utilization rate by 1.44 fold whereas 1.96 fold increase in specific glucose utilization rate were monitored in Pf-5 as compared to the wild type control (Table 5.4).

5.3.4 Effect of *yc* operon genomic integration on citric acid biosynthesis and secretion in fluorescent pseudomonads.

On TRP medium, in presence of 75 mM glucose the organic acid identified were citric acid and gluconic acid. In all *P. fluorescens* strains CHAO-1, ATCC13525 and Fp315 strains, intracellular citrate level by 4.6, 3.16 and 4.45 fold, respectively, as compared to the control strain (Fig. 5.10). However, the intracellular citrate levels were found to be similar in both genomic integrant and plasmid bearing strains. The citrate synthase activity correlated with the intracellular citrate levels. *P. fluorescens* Pf-5(Int) and P109(Int) showed a similar increase in intracellular citrate level by 3.5 and 3.27 fold respectively as compared to the control. Exception of this effect was Pfo-1(Int), in which the intracellular citrate level is 1.3 fold less as compared to Pfo-1(pYC). This data when compared with the respective plasmid bearing strain showed a significant reduction in citrate level by 1.27 and 1.5 fold, respectively. An enhancement of extracellular citrate levels in were achieved in both plasmid bearing and genomic integrants of *P. fluorescens* strains when compared to their respective control *Pf* (pGm) strain (Fig. 5.11; Table 5.5)

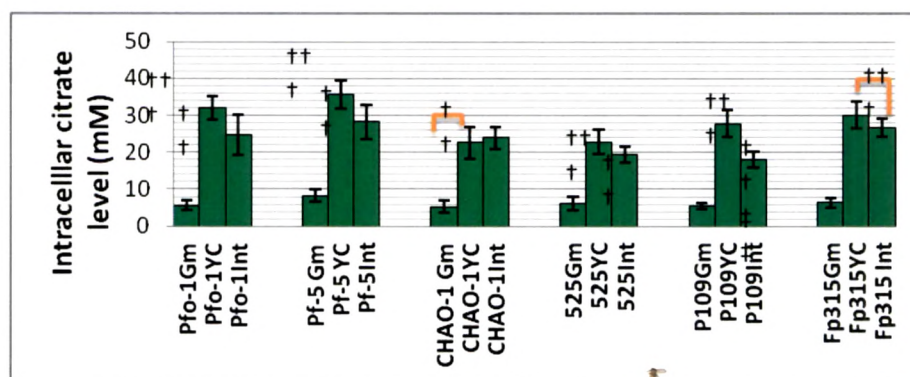


Figure 5.10 : Intracellular citric acid levels in *P. fluorescens* strains *plac yc* genomic integrants. Citric acid levels were estimated from stationary phase cultures grown on 75 mM Tris HCl (pH8.0) rock phosphate (TRP) medium with 75 mM glucose . Results are expressed as Mean \pm S.E.M of 3 independent observations. †comparison of parameters with vector control Gm, ‡ comparison of parameters between pYC plasmid transformants and genomic integrants of fluorescent pseudomonads. †††, ††††, P<0.001; ††, †††P<0.01; †, ‡, P<0.05.

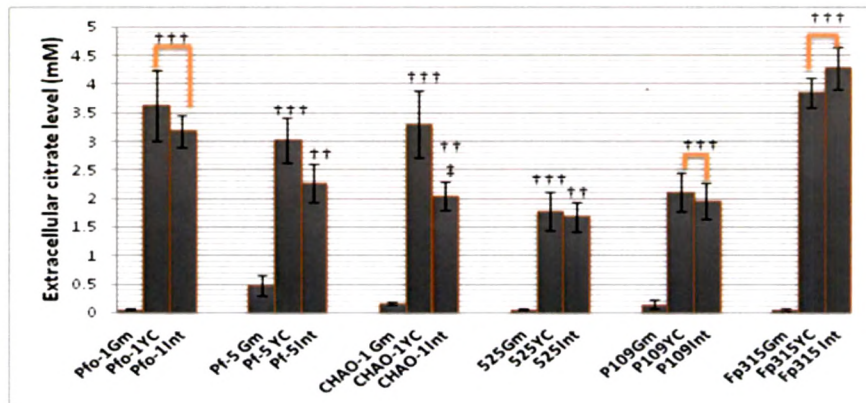


Figure 5.11 : Extracellular citric acid levels in *P. fluorescens* strains *plac yc* genomic integrants. Citric acid levels were estimated from stationary phase cultures grown on 75 mM Tris HCl (pH8.0) rock phosphate (TRP) medium with 75 mM glucose . Results are expressed as Mean \pm S.E.M of 3 independent observations. †comparison of parameters with vector control Gm, ‡ comparison of parameters between pYC plasmid transformants and genomic integrants of fluorescent pseudomonads. †††, ‡‡‡, $P < 0.001$; ††, ‡‡, $P < 0.01$; †, ‡, $P < 0.05$

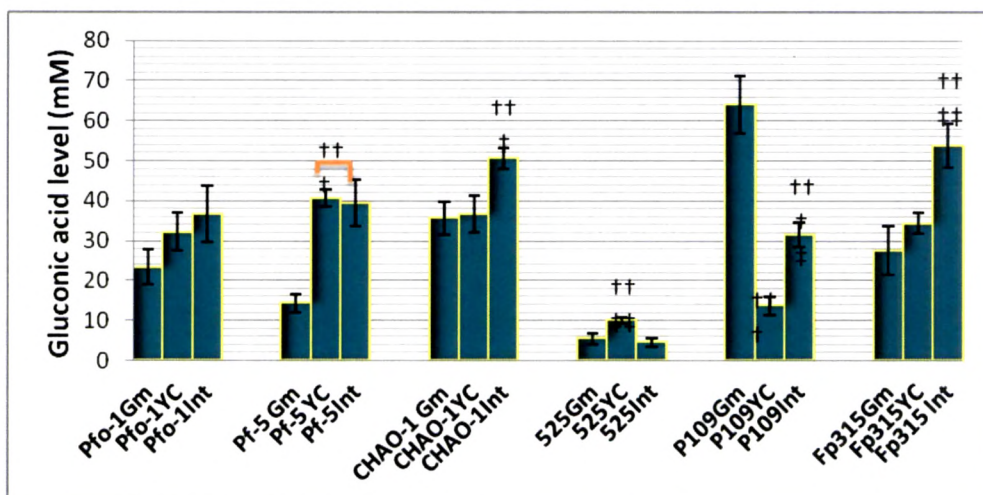


Figure 5.12 : Gluconic acid levels in *P. fluorescens* strains *yc operon* genomic integrants. Gluconic acid levels were estimated from stationary phase cultures grown on 75 mM Tris HCl (pH8.0) rock phosphate (TRP) medium with 75 mM glucose . Results are expressed as Mean \pm S.E.M of 3 independent observations. †comparison of parameters with vector control Gm, ‡ comparison of parameters between pYC plasmid transformants and genomic integrants of fluorescent pseudomonads. †††, ‡‡‡, $P < 0.001$; ††, ‡‡, $P < 0.01$; †, ‡, $P < 0.05$

Table 5.5: Extracellular citrate levels in *P. fluorescens* plasmid bearing strains and genomic integrants of *yc* operon.

<i>P. fluorescens</i> strains	Extracellular citrate level (mM)	Fold increase
PfO-1 (pYC)	3.63±0.62	60
PfO-1(Int)	3.18±0.27	53
Pf-5(pYC)	3.02±0.39	6.4
Pf-5 (Int)	2.26±0.33	4.8
CHAO-1 (pYC)	3.3±0.57	20.6
CHAO-1 (Int)	2.05±0.24	12.8
ATCC13525 (pYC)	1.77±0.34	29.5
ATCC13525 (Int)	1.67±0.26	27.8
P109 (pYC)	2.12±0.35	14.1
P109 (Int)	1.95±0.32	13.0
Fp315 (pYC)	3.86±0.26	77.2
Fp315 (Int)	4.27±0.27	80.5

The values are represented as Mean ±S.E.M of 3 independent observations. The fold increase is calculated in comparison to the extracellular citrate level of *Pf* (pGm) as a control.

The gluconic acid level and GDH activity showed positive correlation amongst the strains (**Table 5.6, Fig. 5.12**).

5.3.5 Alterations in G-6-PDH, CS, ICDH, ICL, PYC, and GDH activities

The effect of genomic integration of *plac yc* gene was also monitored at the level changes of key enzymes involved in periplasmic direct oxidation and intracellular phosphorylative pathways of glucose catabolism along with PYC, participating in anaplerotic reactions of *P. fluorescens* in order to correlate the alterations in physiological variables and organic acid profile. Significant variations were observed amongst the different strains (**Fig. 5.13**).

Table 5.6: Comparison of GDH activity and gluconic acid levels of *P. fluorescens* plasmid bearing strains and genomic integrants of *yc* operon.

<i>P. fluorescens</i> strains	GDH activity nmole/min/mg protein	Gluconic acid level (mM)	GDH activity fold increase/decrease	Gluconic acid level-fold increase/decrease
PfO-1 (pYC)	54.4±5.4ns	32.2±4.79 ns	1.6	1.38
PfO-1(Int)	76.3±8.5 ††	36.7±6.95 ns	2.25	1.57
Pf-5(pYC)	91.3±4.4 ††	40.7±2.2 †††	1.69	2.83
Pf-5 (Int)	103.2±9.1††	39.5±5.65 †††	1.91	2.74
CHAO-1 (pYC)	23.5±3.7 ns	36.7±4.45 ns	UD	UD
CHAO-1 (Int)	73.07±10.6 †††	50.6±2.56 ††	2.7	1.42
ATCC13525 (pYC)	63.1±9.3 ns	10.04±0.67 ††	UD	1.8
ATCC13525 (Int)	43.5±6.6 ns	4.54±0.97 ns	1.4 decrease	1.2 decrease
P109 (pYC)	26.2±8.2 †††	13.8±2.33 †††	3.3 decrease	4.6 decrease
P109 (Int)	37.5±5.6 †††	31.4±3.01 †††	2.32 decrease	2.04 decrease
Fp315 (pYC)	73.8±9.1 †††	34.3±2.6 ns	2.11	1.27
Fp315 (Int)	79.2±8.3 †††	53.8±5.5 ††	2.26	1.99

The values are represented as Mean ±S.E.M of 3 independent observations. The fold increase is calculated in comparison to the extracellular citrate level of *Pf* (pGm) as a control. UD signifies undetectable, †comparison with *Pf* (pGm). ††† $p < 0.001$, †† $p < 0.01$, † $p < 0.05$, ns $p > 0.05$.

All genomic integrants showed no alteration in ICDH and ICL activities with an exception of Pf-5 (pYC) and Pf-5 (Int) which showed an increase in ICDH activity by 1.7 fold and ICL activity by 2.7 fold, respectively, as compared to wild type strain. Interestingly,

majority of genomic integrants of *yc* operon showed CS activity at par with the plasmid transformants. The CS activity is increased by 3.17 and 2.64 fold in *P. fluorescens* Pfo-1 *yc* operon genomic integrant and plasmid bearing strains, respectively. Similarly, the increase was 4.73 and 4.6 fold in Pf-5, 4.1 and 2.7 fold in CHAO-1, 6 fold each in ATCC13525, 1.9 and 2.2 fold in P109 and 3.4 and 2.65 fold in Fp 315 as compared to the respective wild type controls. Remarkably, the CHAO-1 genomic integrant showed 1.5 fold higher CS activity than that of CHAO-1(pYC) strain. Both plasmid bearing strain and genomic integrants showed a decrease in G6PDH activity which indicates the diversion of glucose flux more towards the direct oxidation pathway.

50% reduction in G6PDH activity was observed in both Pfo-1 (Int) and Pfo-1(pYC) as compared to control. Similarly, the fold decrease in other strains are 11.7 and 8.9 fold in Pf-5, 1.94 and 5.6 fold in ATCC 13525, 1.8 and 1.6 fold in Fp315 were observed in this enzyme activity. Unlike the other strains, CHAO-1 showed a significant enhancement of G6PDH activity by 3 fold as compared to the vector control.

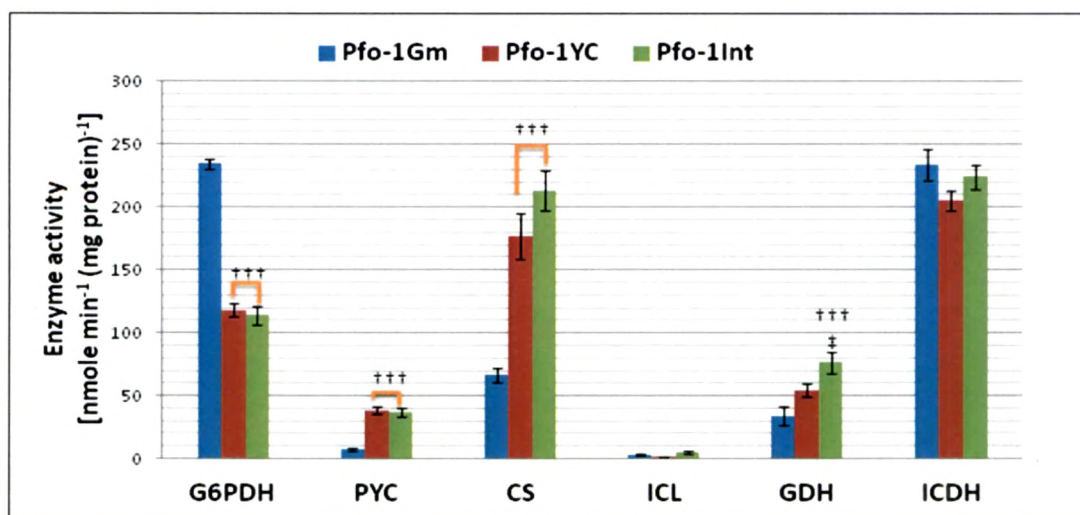


Figure 5.13: Activities of enzymes G-6-PDH, ICDH, ICL, PYC, and GDH in *P. fluorescens* Pfo-1 *yc* operon genomic integrants. The activities have been estimated using vector control *Pf* (pGm), plasmid transformants of *Pf* (pYC) and *yc* operon genomic integrants. Cultures were grown on TRP minimal medium

with 75 mM glucose. All the enzyme activities were estimated from mid log phase to stationary phase cultures and are represented in the units of nmoles/min/mg total protein. The values are depicted as Mean \pm S.E.M of 3 (N=3) independent observations. †comparison of parameters with vector control Gm, ‡ comparison of parameters between pYC plasmid transformants and genomic integrants of fluorescent pseudomonads. †††,‡‡‡,P<0.001; ††,‡‡P<0.01; †,‡,P<0.05.

The percentage change in G6PDH activity were correlated with Change in GDH activity. GDH activity increased by 2.6 fold in PfO-1(Int),1.9 fold Pf-5(Int),2.74 fold in CHAO-1(Int), 2.6 fold in Fp315(Int) as compared to the reselective control strain.A significant decrease in GDH activity observed in ATCC13525(Int) (1.4 fold) and P109(Int) (2.76 fold) as compared to the control. PYC activity remain unaltered in *P. fluorescens* PF-5,CHAO-1, P109 and Fp315 genomic integrants whereas an increase by 5 fold and 2.8 fold in *P. fluorescens* PfO-1(Int) and ATCC13525(Int) respectively were observed compared to control (Fig 5.14-5.18).

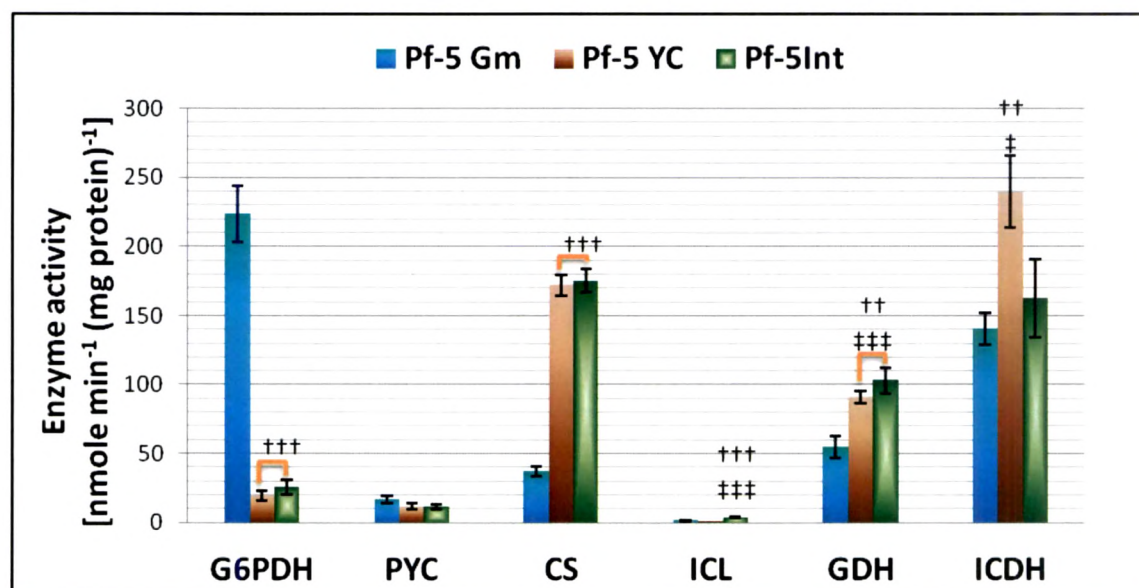


Figure 5.14: Activities of enzymes G-6-PDH, ICDH, ICL, PYC and GDH in *P. fluorescens* Pf-5 *yc* operon genomic integrants. The activities have been estimated using vector control *Pf*(pGm), plasmid transformants of *Pf* (pYC) and *yc* operon genomic integrants. Cultures were grown on TRP minimal medium with 75 mM

glucose. All the enzyme activities were estimated from mid log phase to stationary phase cultures and are represented in the units of nmoles/min/mg total protein. The values are depicted as Mean \pm S.E.M of 3 (N=3) independent observations. †comparison of parameters with vector control Gm, ‡ comparison of parameters between pYC plasmid transformants and genomic integrants of fluorescent pseudomonads. †††, ‡‡‡, P<0.001; ††, ‡‡P<0.01; †, ‡, P<0.05.

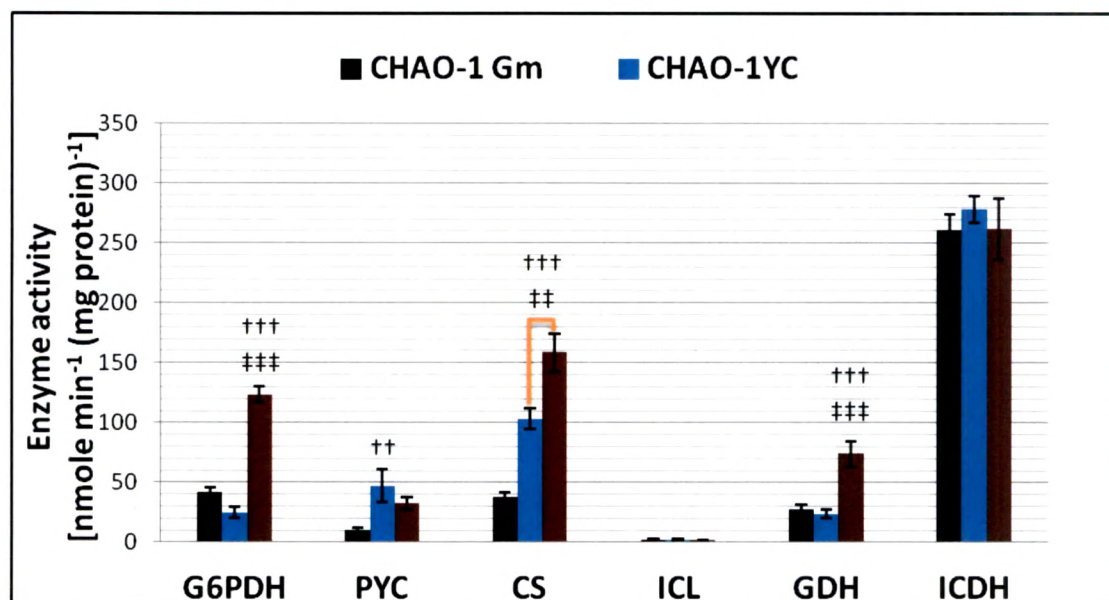


Figure 5.15: Activities of enzymes G-6-PDH, ICDH, ICL, PYC, and GDH in *P. fluorescens* CHAO-1 *yc* operon genomic integrants. The activities have been estimated using vector control *Pf* (pGm), plasmid transformants of *Pf* (pYC) and *yc* operon genomic integrants. Cultures were grown on TRP minimal medium with 75 mM glucose. All the enzyme activities were estimated from mid log phase to stationary phase cultures and are represented in the units of nmoles/min/mg total protein. The values are depicted as Mean \pm S.E.M of 3 (N=3) independent observations. †comparison of parameters with vector control Gm, ‡ comparison of parameters between pYC plasmid transformants and genomic integrants of fluorescent pseudomonads. †††, ‡‡‡, P<0.001; ††, ‡‡P<0.01; †, ‡, P<0.05.

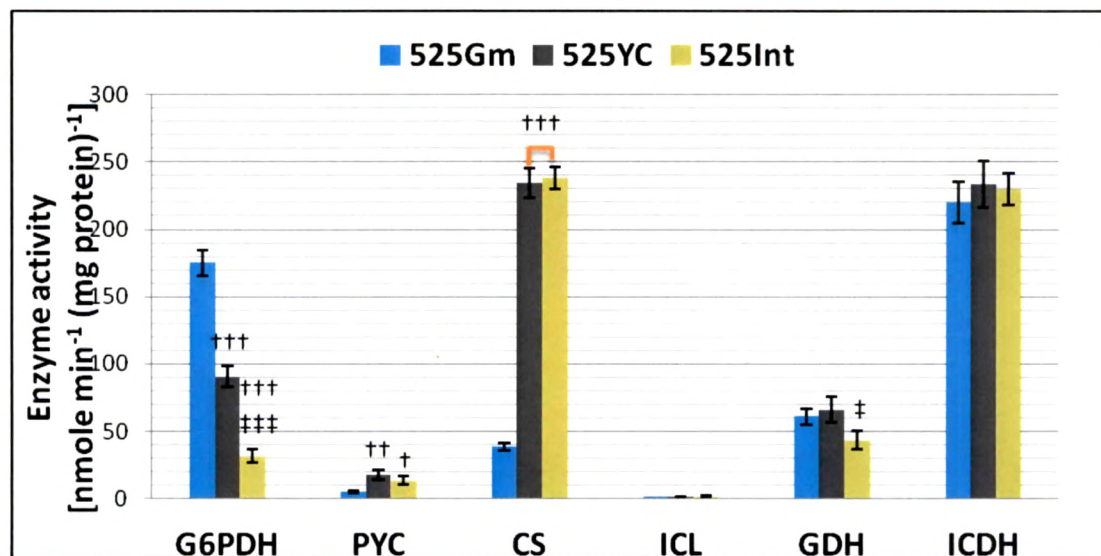


Figure 5.16: Activities of enzymes G-6-PDH, ICDH, ICL, PYC, and GDH in *P. fluorescens* ATCC 13525 *yc* operon genomic integrants. The activities have been estimated using vector control *Pf* (pGm), plasmid transformants of *Pf* (pYC) and *yc* operon genomic integrants. Cultures were grown on TRP minimal medium with 75 mM glucose. All the enzyme activities were estimated from mid log phase to stationary phase cultures and are represented in the units of nmoles/min/mg total protein. The values are depicted as Mean \pm S.E.M of 3 (N=3) independent observations. †comparison of parameters with vector control Gm, ‡ comparison of parameters between pYC plasmid transformants and genomic integrants of fluorescent pseudomonads. †††, ‡‡‡, $P < 0.001$; ††, ‡‡, $P < 0.01$; †, ‡, $P < 0.05$

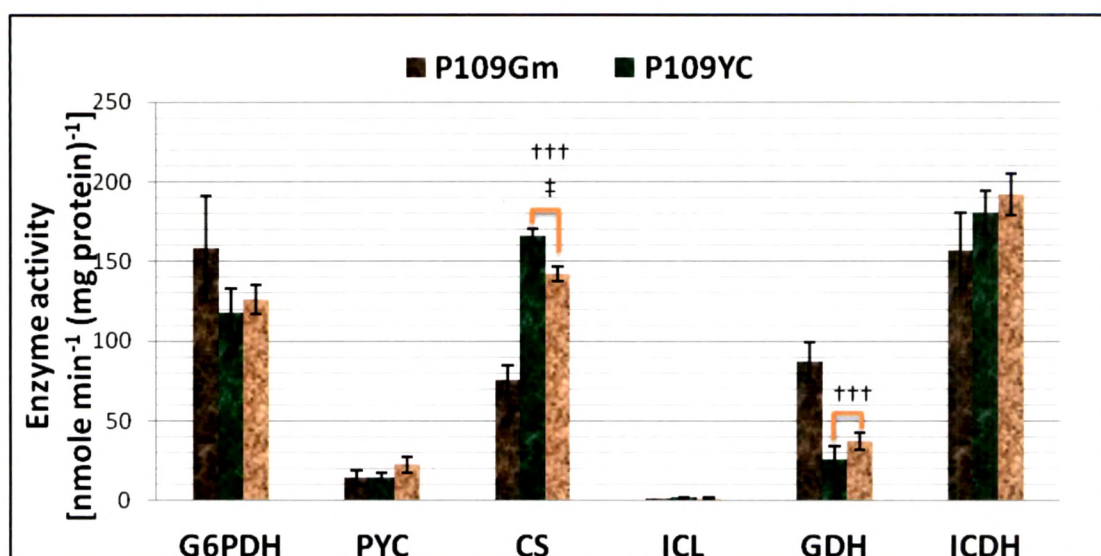


Figure 5.17: Activities of enzymes G-6-PDH, ICDH, ICL, PYC, and GDH in *P. fluorescens* P109 *yc* operon genomic integrants. The activities have been estimated using vector control *Pf* (pGm), plasmid transformants of *Pf* (pYC) and *yc* operon genomic integrants. Cultures were grown on TRP minimal medium with 75 mM glucose. All the enzyme activities were estimated from mid log phase to stationary phase cultures and are represented in the units of nmol/min/mg total protein. The values are depicted as Mean \pm S.E.M of 3 (N=3) independent observations. †comparison of parameters with vector control Gm, ‡ comparison of parameters between pYC plasmid transformants and genomic integrants of fluorescent pseudomonads. †††, ††††, P<0.001; ††, †††P<0.01; †, ‡, P<0.05

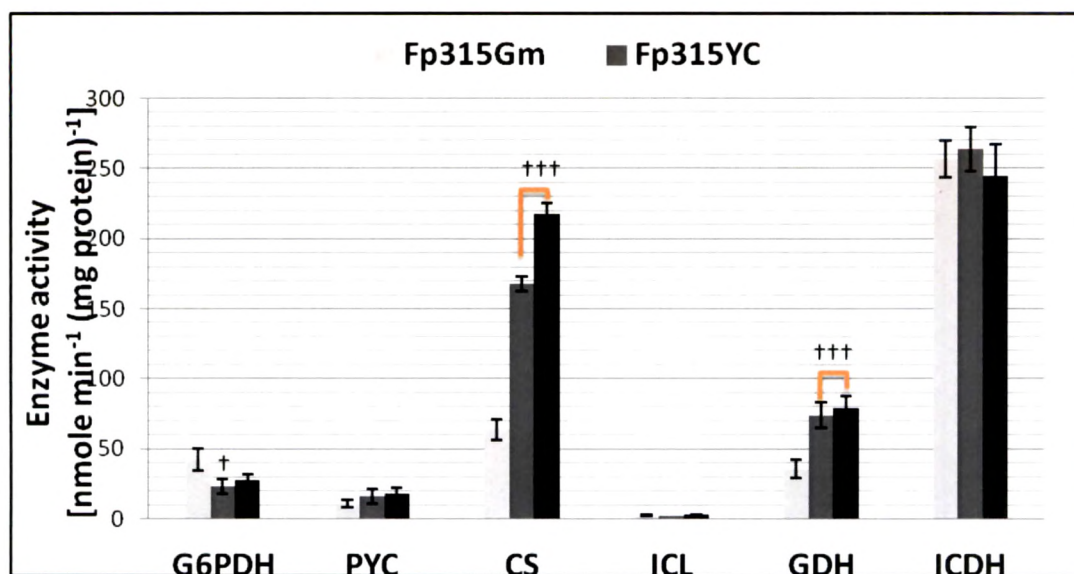


Figure 5.18: Activities of enzymes G-6-PDH, ICDH, ICL, PYC, and GDH in *P. fluorescens* Fp 315 *yc* operon genomic integrants. The activities have been estimated using vector control *Pf* (pGm), plasmid transformants of *Pf* (pYC) and *yc* operon genomic integrants. Cultures grown on TRP minimal medium with 75 mM glucose. All the enzyme activities were estimated from mid log phase to stationary phase cultures and are represented in the units of nmoles/min/mg total protein. The values are depicted as Mean \pm S.E.M of 3 (N=3) independent observations. †comparison of parameters with vector control Gm, ‡ comparison of parameters between pYC plasmid transformants and genomic integrants of fluorescent pseudomonads. †††, ††, †‡P<0.001; ††, †‡P<0.01; †, ‡, P<0.05

5.4 Discussion

Genetic engineering of microorganisms involves the use of extra-chromosomal plasmid for heterologous expression of desired genes. Plasmid DNA is known to cause metabolic burden on the cell and alter its metabolism depending on the host organism, plasmid nature, and environmental conditions (Buch et al., 2010b; Sharma et al., 2011). Hence the genetic manipulations need be directed to the chromosomal integration as it would lead not only to increased stability but also decrease the metabolic load caused by the presence of the plasmids to nullify the pleiotropic effects on the host metabolism. The present study demonstrates the effect of genomic integration of *E. coli* NADH insensitive *cs* Y145F gene and *S. tphilimurium citC* gene on fluorescent pseudomonads. Previous chapters

describe the effect of heterologous overexpression on M9 minimal media. The study is an attempt to describe the following aspects on phosphate deficient buffered media: 1) Effect of genomic integration of heterologous gene on *P. fluorescens* physiology and glucose metabolism, (2) comparison of the effects of similar genetic modification between the plasmid transformants and genomic integrants of the same strain. (3) Comparison of the effect of similar genetic modification on different strains of PGPR fluorescent pseudomonads including natural isolates.

Remarkably, CS activity in genomic integrants remain unaltered as compared to the plasmid based expression with mid copy number plasmid pUCPM18 Gm. In addition, *P. fluorescens* CHAO1 genomic integrants showed 35% improvement on CS activity. Similar study carried out wherein gene encoding polyphosphate kinase (PPK) were overexpressed using low copy mini F plasmid as well as multicopy pMB1 based plasmid (Carrier et al., 1998) in *E. coli* DH10B strain. PPK activity with low copy plasmid caused a 20 fold increase in polyphosphate (poly P) content in the early stage of growth whereas the enhancement was 80% in the stationary phase. The profile using multicopy plasmid depicted a different behavior of product content per cell versus culture time. PolyP increased dramatically within the first 3 h; however, the high product-levels were not maintained in stationary phase. At 24 h, the polyP levels were the same as those obtained using a low-copy plasmid, dropping to one-fourth of that observed at 3 h (Jones et al., 2000)

Our result was in consistent with the above study. The whole study indicate that overexpression of gene using plasmid could alter the energy status of the cell such that overall productivity may be compromised. The extra resources of the cell is diverted toward recombinant protein synthesis from a multicopy plasmid can severely burden the host cell, as indicated by the slow growth rate of the multicopy plasmid-bearing strain. Genomic integrants thus play a role in overcoming these obstacles